

Enzyme Kinetics in Crowded Cellular Environment

GUI-NA WEI and QING-LING ZOU*

Department of Nephrology, Second Affiliated Hospital, School of Medicine, Zhejiang University, Hangzhou 310008, P.R. China

*Corresponding author: E-mail: qlzhou72@163.com

(Received: 19 December 2011;

Accepted: 25 April 2012)

AJC-11269

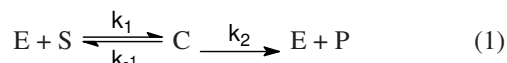
This study reports, the Michaelis-Menten scheme of enzyme-network kinetics in crowded environment based on a particle-based stochastic model. The effects of crowding, cooperative reaction from enzyme-network and size of substrates are investigated. The diffusion behaviour is computed and compared under different obstacle volume fraction and different size of substrate. We find the crowded environment embedded in enzyme-network greatly increases the compartmentalization of substrate with big size, leading to the obvious increase of probability of rebind of released substrate to its initial enzyme and decrease to other enzymes. When volume fraction of obstacle is increased, the survival probability of small substrate is decreased while it increases in big substrate case. Time dependent reaction rate coefficient is studied in different time scale.

Key Words: Enzyme-network, Crowded cellular environment, Particle-based stochastic model.

INTRODUCTION

In living cells, the cytoplasmic environment is quite different from that usually encountered *in vitro*. Intracellular environments are highly crowded due to the presence of various bio-macromolecules, which may occupy a large volume fraction of the cell, typically ranging from 10 to 40 % of the total cellular volume^{1,2}. Crowding leads to various relevant effects, such as thermodynamic and kinetic effects, on the properties of reagents. For example, the crowding decreases the diffusion of protein and enhances relevant protein association³, self-association of monomers⁴ and increases the rate of folding and refolding⁵.

In biochemistry, the Michaelis-Menten (Michaelis-Menten) scheme of enzyme kinetics is a paradigmatic model. It consists of a set of three elementary chemical reactions: A substrate, S, binds reversibly to an enzyme, E, forming enzyme-substrate complex, C, that undergoes unimolecular decomposition to form a product, P and the original enzyme:



where, k_i is the rate coefficient associated with the elementary step i . The Michaelis-Menten reaction kinetics is strongly influenced by diffusion of reactants. The phenomena are dramatically changed when the media become crowded. In low-dimensional and fractal systems such as biological membrane, diffusion is not a perfectly mixing process^{2,6-9}. The crowded system shows anomalous sub-diffusion, which is characterized by mean

displacement of the molecule $\langle R^2(t) \rangle \propto t^\alpha$ with $\alpha < 1.0$. Consequently, fractal kinetics displays $k_i(t) = k_i(0)t^h$ with h fractal exponent and pronounced substrate-product segregation⁶. However, the kinetics of Michaelis-Menten reaction in crowding three-dimensional (3D) system embedded in enzyme-network which displays cooperative reaction are still open.

Intracellular environments is very complex. The size of substrate molecules is distinct in different system. Even in one cell, different species of substrate molecules have distinct size. The Michaelis-Menten reaction kinetics may be influenced by the size of substrate molecules. For example, the Michaelis constant K_M value of EcoRI depends sensitively on the size of the substrate¹⁰. Small substrate molecules which are generally treated as point particles in many documented studies¹¹⁻¹⁴ can diffuse into any free space. The main influences of crowded environment is blocking its free diffusion. However, some substrates have comparable sizes to the obstacles. In this case, the diffusion of substrates with big size is limited by the crowded background greatly. Due to the volume exclusion effect, it can not enter into space between obstacles with size smaller than itself. Consequently, the crowded obstacles may compartmentalize the big substrates, which not only decreases the diffusion coefficient but also results in many other effects, such as reaction noise from low copy number of molecules in compartments^{15,16}, increase of the rate of re-collision¹⁷ and soon. Consider system consists of enzyme network embedded in crowded environment, the kinetics of Michaelis-Menten reaction will be greatly enriched.

EXPERIMENTAL

Simulation model: Slow diffusion rates in combination with complicated environments make classical mean-field description by mass law is invalid, which make it necessary to make use of stochastic model *in vivo* biochemistry. Many methods have been employed to simulate reversible reaction in this field, including Brownian dynamics^{11,17}, Monte Carlo simulation⁶, molecular dynamics (MD)^{18,19} and *etc.* In our model, a particle-based stochastic model based on a mesoscopic hybrid molecular dynamics-multiparticle collision (MD-MPC) dynamics scheme is put forward to simulate Michaelis-Menten kinetics.

We consider a 3D cubic system with volume V employing periodic boundary condition. In the initial state, the system contains four species of molecules, *i.e.* substrates (with number N_S , mass m_S and radius r_S), obstacles (with number N_O , mass m_O and radius r_O), enzymes (with number N_E , mass m_E and radius r_E) and point-like solvent molecules (with number N_M and mass m_M). Their initial positions are randomly distributed with the condition that they do not overlap on to each other and velocities obey Maxwellian distribution. The enzymes and enzyme-substrate complexes interact with each other and with the obstacle, solvent, substrate and product molecules through repulsive Lennard-Jones (LJ) potentials.

$$V_{LJ}(r) = 4 \epsilon \left[\left(\frac{r_E}{r} \right)^{12} - \left(\frac{r_E}{r} \right)^6 + \frac{1}{4} \right], \quad r > r_c \quad (2)$$

where, $r_c = 2^{1/6} r_E$ is a cut-off distance. The time evolution of the non-reaction process is carried out using a mesoscopic hybrid molecular dynamics-multiparticle collision (MD-MPC) dynamics scheme³, which consists of a streaming step and a collision step. In the streaming step (molecular dynamics step), within a time interval τ_{MD} , the motions of all particles are governed by Newton's equations of motion. In the collision step (MPC step), within a time interval τ_{MPC} , multiparticle collisions occur among the solvent, product and substrate molecules. To carry out multiparticle collision, the system is divided into many cubic cells with size a_0 . Collisions occur independently in each cell. The post-collision velocity v'_i of each particle i in a cell I , relative to the center-of-mass velocity $V_{cm} = \sum_{i=1}^{N_I} V_i$, where N_I is the instantaneous number of particles in cell I , is rotated with respect to a randomly chosen unit axis by a fixed angle θ ,

$$v'_i = V_{cm} + \omega_i(\theta)(v_i - V_i) \quad (3)$$

where, $\omega_i(\theta)$ is a random rotation matrix operator. Since the hybrid dynamics is microcanonical, preserving mass, momentum and energy conservation, phase space volumes, all important characteristics of full molecular dynamics. In recent simulation, MPC algorithms has widely applied to study colloid and polymer dynamics²⁰, the behaviour of vesicles and cells in hydrodynamic flows and the dynamics of viscoelastic fluids²¹ and chemical propelled nanomotor²².

Once n substrate molecules diffuse into the reaction zone ($r < r_c$) of enzyme in one MD step, one substrate will randomly be picked up to participate the reaction $E + S \rightarrow C$ with probability $p_R = 1 - (1-p)^n$ with p the probability of reaction of a substrate-enzyme pair. Once a complex is formed at time t ,

we assume the disassociation takes place in the time $t + 1/(k_2 + k_0^{-1}) \ln(1/R_1)$ based on Gillespie's method²³, where R_1 is a random number. If $R_2 < k_2/(k_2 + k_0^{-1})$ (R_2 is another random number), the reaction $C \rightarrow E + P$ will occur, otherwise the reaction is $C \rightarrow E + S$.

In the simulation of Michaelis-Menten reaction mentioned above, we make use of a rule conserving the mass, momentum and energy of the system²⁴. For the reaction $E + S \rightarrow C$, the formed velocity of complex can be obtained based on mass and momentum conservation,

$$v_C = (m_E v_E + m_S v_S) / m_C \quad (4)$$

where, $m_C = m_E + m_S$ is the mass of the complex. It is impossible to conserve energy without any other molecules participating in this process. To avoid this point, it is necessary to flow the surplus energy into the solution, which may act as heat bath. Two solvent molecules near the reacting enzyme are randomly picked up to receive the surplus energy. Consider that these two solvent molecules should also satisfy momentum conservation, the post velocities of these two solvent molecules are:

$$\begin{aligned} v'_{M1} &= \frac{1}{2}(v_{M1} + v_{M2}) + \frac{1}{2} \hat{n}_1 v'_{Mr} \\ v'_{M2} &= \frac{1}{2}(v_{M1} + v_{M2}) + \frac{1}{2} \hat{n}_1 v'_{Mr} \end{aligned} \quad (5)$$

where,

$$v'_{Mr} = \left(\frac{2\mu_{ES}}{m_M} v_r^2 + \frac{4}{m_M} v_{ES}(r_{ES}) + v_{Mr}^2 \right)^{1/2} \quad (6)$$

Here $m_{VMr} = v_{M1} - v_{M2}$ is the relative velocity of the two solvent molecules, \hat{n}_1 is a randomly chosen unit vector, $v_r = v_E - v_S$, $r_{ES} = r_E - r_S$ and $\mu_{ES} = m_E m_S / (m_E + m_S)$. For the reaction $C \rightarrow E + S$ (or P), the substrate (or product) is released outside of the reaction surface of enzyme and get energy from the solution. Again, two solvent particles near the decomposing complex are picked up to participate this process. The post-reaction velocities of solvent particles are taken to be

$$V'_{Mj} = \frac{1}{2}(v_{M1} + v_{M2}), \quad j = 1, 2 \quad (7)$$

For the enzyme and substrate molecules, their post-reaction velocities are

$$\begin{aligned} V'_E &= v_C + \frac{m_S}{m_C} \sqrt{\frac{m_M}{2\mu_{ES}}} \hat{r}_{SE} v_{Mr} \\ V'_S &= v_C - \frac{m_E}{m_C} \sqrt{\frac{m_M}{2\mu_{ES}}} \hat{r}_{SE} v_{Mr} \end{aligned} \quad (8)$$

where, \hat{r}_{SE} is a unit vector pointing from E to S . Since the velocity of solvent particles obey Maxwellian distribution, it is checked that the post velocity of released substrates (or product) also shows Maxwellian distribution characterized by system temperature. Thus, reactive collisions are constructed to conserve mass, momentum and energy and account for energy transfers to and from the surrounding solvent molecules that serve as heat bath. Also, the rule ensure that the reversible reaction steps satisfy detailed balance. The detail description of this rule has been introduced in reported work²⁴.

All quantities are reported in dimensionless LJ units in this paper. Distances and energy are measured in units of r_E and ϵ , temperature in units of ϵ/k_B and time in units of

$r_E \sqrt{m/\epsilon}$. The simulations were carried out on systems containing $V = L^3 = 30^3$ MPC cells with unit volume. The rotation operators in the MPC dynamics were chosen to describe rotations by $\theta = 90^\circ$ about randomly chosen axes. The temperature was determined from the average kinetic energy. We set $N_E =$

100 and $\rho_M = 8.0 \left(\rho_M = \frac{N_M}{V - 4(N_O r_O^3 + N_E r_E^3)\pi/3} \right)$, which is

the density of solvent molecules. The density of substrate ρ_S is $= \frac{N_S}{V - 4(N_O r_O^3 + N_E r_E^3)\pi/3}$. The volume fraction of obstacle

is defined by $\phi = N_O \frac{4\pi r_O^3}{3V}$ (small volume fraction of enzymes is neglected). The radius of enzyme, complex and obstacle is

fixed to be 1.0. The mass of enzyme and obstacle is $\rho_M \frac{4\pi r_E^3}{3}$.

The temperature of system is set to be $K_B T = 0.2$. In order to focus on the influences of substrate diffusion on crowded Michaelis-Menten kinetic, we set the mass of substrate to be 1 (identical with solvent particles) while its radius is changed so that it can diffuse fast to explore the environment background. The MD time step used to integrate Newtons equations of motion with the velocity Verlet algorithm is $\tau_{MD} = 0.001$, while the multiparticle collision time is 1.0.

The conservations of mass, momentum and energy in the system are ensured since they are satisfied both in non-reaction dynamics and in reaction kinetics. An example displaying the evolution of energy is presented in Fig. 1, where one can find that the fluctuation is very small. Thus, important general features of full molecular dynamics are preserved in this mesoscopic model, which make the hydrodynamic interactions properly accounted for and additional assumptions about friction coefficients or random forces not required.

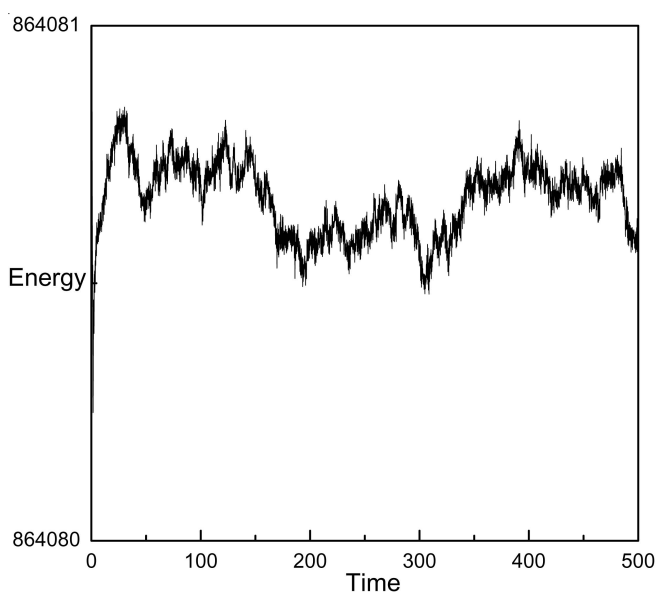


Fig. 1. Evolution of energy in Michaelis-Menten system with volume $V = 60^3$ containing 100 enzymes, 3000 substrates, 100 obstacles and 1.728×10^6 solvent molecules. The reaction parameter is: $k_2 = 0.5$, $k_{-1} = 0.01$

RESULTS AND DISCUSSION

Firstly, in order to investigate the Michaelis-Menten kinetics when the system is crowded by obstacles, we compute the dependence of diffusion coefficient on the volume fraction of obstacles. It is shown in Fig. 2(a) that the value of $D(\phi)$ decreases with increasing volume fraction when the substrates are treated as point-like particles. When the value of ϕ is increased to 0.3, the diffusion coefficient is decreased about 40%. In MPC, an approximate analytical expression for the diffusion coefficient can be expressed by expression²⁵

$$D_0 = \frac{K_B T \tau_{MPC}}{2m} \left(\frac{3\rho^s}{(\rho^s - 1 + e^{-\rho^s})(1 - \cos\theta)} - 1 \right) \quad (9)$$

From this expression, one can get $D = 0.28$ if obstacles are absent which is exactly the value we get from simulation. Since the obstacles are distributed randomly, the theoretical expression of $D(\phi)$ can be obtained from evolution equation for the density field²⁶.

$$D(\phi) = D_0 \frac{1 + \phi}{1 - \phi/2} \quad (10)$$

We compare the dependence from this function with that from simulation in Fig. 1(a). One can see they show perfect agreement.

The diffusion coefficient is plotted from mean square displacement $\langle R^2(t) \rangle$. In Fig. 2(b), we show $\langle R^2(t) \rangle$ with different radius of substrate molecules. In the short time, the substrates show ballistic motion with fast increase of $\langle R^2(t) \rangle$. Then, it undergoes different dynamics regime depending on the radius of substrate. For small r_s , it quickly enter into normal diffusion regime showing $\langle R^2(t) \rangle = 6Dt^\alpha$ with $\alpha = 1.0$. Small substrate can explore almost any unoccupied volume between obstacles while big substrate can not diffuse into space smaller than its size. Thus, for big r_s , it shows an subnormal diffusion regime $\langle R^2(t) \rangle \propto t^\alpha$ with $\alpha < 1.0$ after the ballistic regime. From the series of curves, one can find this point. Following this regime in the long time, the diffusion enters into normal regime again. In low-dimensional system, fractal structure from crowded environment may result in obvious sub-diffusion⁶. We present the diffusion coefficient with $r_s = 1.0$ in Fig. 2(a). It is shown that the decreases of $D(\phi)$ is pronounced as ϕ is increased, displaying strong nonlinearity. Beyond $\phi = 0.3$, it is very difficult for the substrate to diffuse in the crowded background. Two aspects from crowded environment, namely, increase of volume fraction of obstacles and consequent decrease of spaces for big substrate to explore among obstacles, leads to the dramatic decrease in $D(\phi)$. The increase of r_s distinctly decreases the diffusion coefficient for the latter reason, which is show in Fig. 2(c).

System consisting of many enzymes forms a reaction network, which shows cooperative behaviour. Thus, it may exhibit different kinetic behaviour from that in system with only one enzyme. When a complex is formed in Michaelis-Menten reaction, it may disassociate into enzyme and a substrate again or generating a product. The released substrate has two fates: one is that it associates with the initial enzyme again, which is called self-rebind; in contrast to one enzyme system, it may diffuse away from its initial enzyme and subsequently

forms complex with other enzyme, which is called other-rebind. It is sure that the increase of volume fraction of obstacle will decrease the probability of first collision between enzyme and substrate and other-rebind since the diffusion of substrate is blocked by these obstacles. On the other hand, the crowded environment compartmentalizes the system, which increases the probability of self-rebind. The decrease of the first-collision and self-rebind accordingly decreases the reaction rate while the other-rebind increases it. Thus, whether the reaction rate is increased or not depends on what effects play the dominative role.

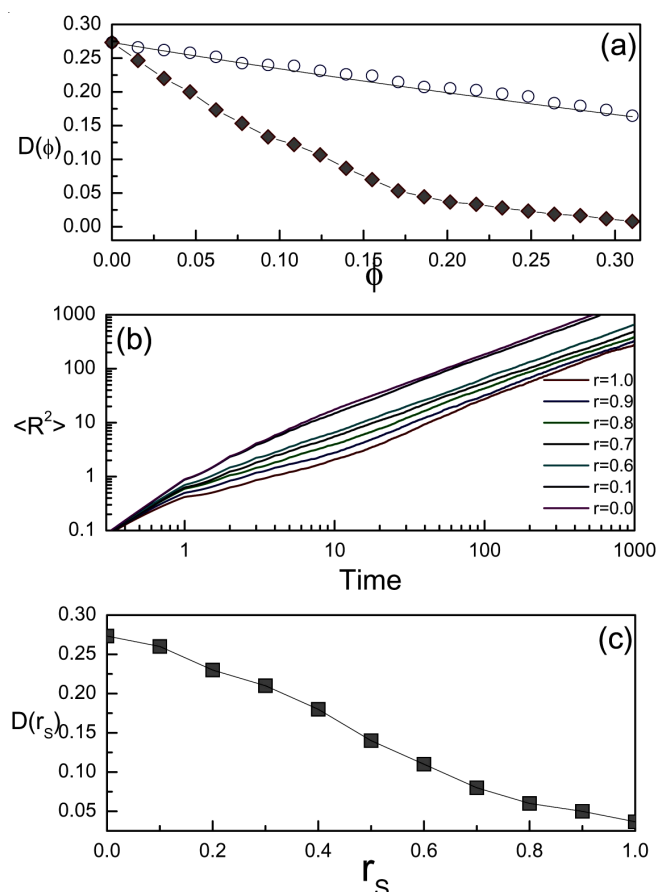


Fig. 2. (a) Dependence of diffusion coefficient D on obstacle volume fraction ϕ with $r_s = 0$ (circles) and $r_s = 1.0$ (squares). The solid line is plotted from eqn. (9); (b) Mean squared displacement $\langle R^2 \rangle$ of the substrate is plotted as a function of time with different r_s ; (c) Diffusion coefficient as a function of r_s with $\phi = 0.2$

In Fig. 3(a,b), the dependence of rebind probability on volume fraction of obstacle is presented. It is shown that the probability of the self-rebind P_S is increased with ϕ . The increase is quite pronounced when the radius of substrate is big since the compartmentalization is more obvious. For the same causation, the other-rebind probability P_O is decreased fast with increasing of ϕ when the size of substrate is big. Thus, the total probability of rebinding is not increased much. In recent work, the system containing one enzyme is simulated by Brown dynamics and analyzed based on Smoluchowski theory¹⁷. In this simulation, the size of enzyme, substrate and obstacle are all identical, which is similar with our case with big substrate. They reported that the reaction rate is decreased when the value of ϕ is increased if reaction probability is 1.0. The probability

of reaction p in $E + S \rightarrow C$ is $p = 1.0$ in our simulation. The great decrease of $D(0.3)$ leads to predominating of first collision. Thus, the reaction rate is decreased when ϕ is increased, which is confirmed in Fig. 4(a), where the survival probability P_L of substrate is plotted. Our simulation is in accord with the reported result¹⁷. If the probability of reaction $E + S \rightarrow C$ is very small (0.001), the recollision predominates. Consequently, it seems that the reaction rate as well as P_S will increase with ϕ quickly, especially in the case with big substrate. However, consider the reaction network consisting of many enzymes, the effect of substrates compartmentalization from crowded obstacles also decrease the probability of other rebind P_O [Fig. 3(b)] and the increase of total probability of recollision to enzyme is small [Fig. 3(c)]. Therefore, the increase of reaction rate with small p in enzyme-network is not easy to be obtained, especially compared to system containing one enzyme. Our direct simulation also confirms this point.

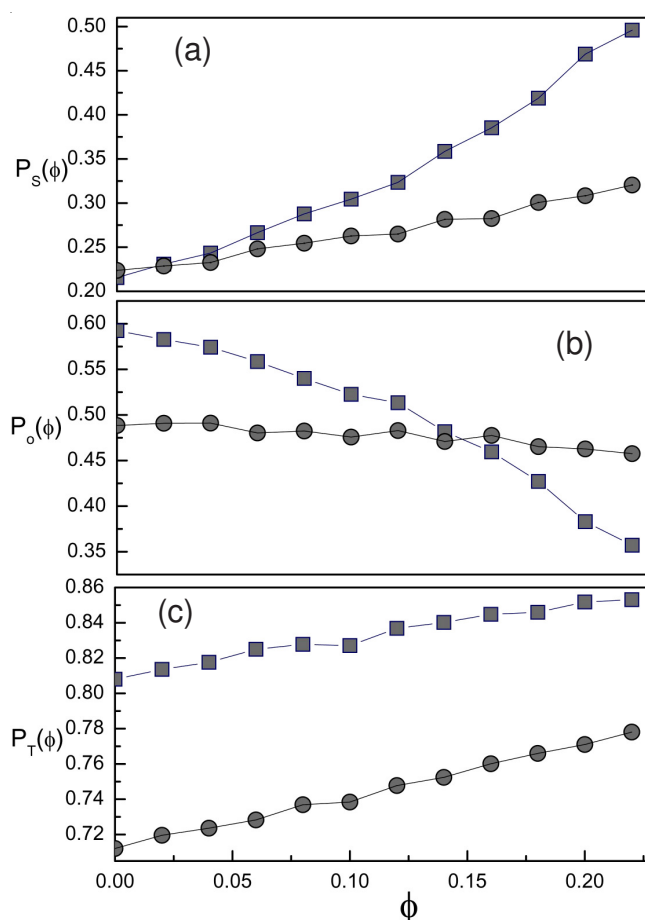


Fig. 3. Rebinding probability of released substrates with big size ($r_s = 1.0$, squares) and small size ($r_s = 0$, circles) to enzymes. (a) To initial enzymes (P_S). (b) To other enzymes (P_O). (c) Total probability (P_T) of rebinding. The reaction rate is $k_2 = 0.01$ and $k_{-1} = 0.5$. The data is plotted from 24 realization at $t = 500$

Different from the case with big size substrate, we find the survival probability P_L of substrate with small size decreases as ϕ is increased, which is illustrated in Fig. 4(b). Thus, the value of P_L is also influenced by radius of substrate. With $p = 1.0$, the first collision determined by diffusion coefficient dominates the reaction $E + S \rightarrow C$. However, compared to the case with big substrate, it has been shown in Fig. 2(a) that the

decrease of diffusion of small substrate is not large. On the other hand, strong deviation of substrate distribution from uniformity appears as the global volume fraction of obstacles increases. In Fig. 4(c), it is shown that the local density of substrates near enzyme in crowded system with $\phi = 0.3$ is much higher than that with $\phi = 0$. The increased first collision resulted from high local density of substrate covers the decreased first collision from the not-small diffusion coefficient. As a consequence, the different P_L dependence on substrate radius.

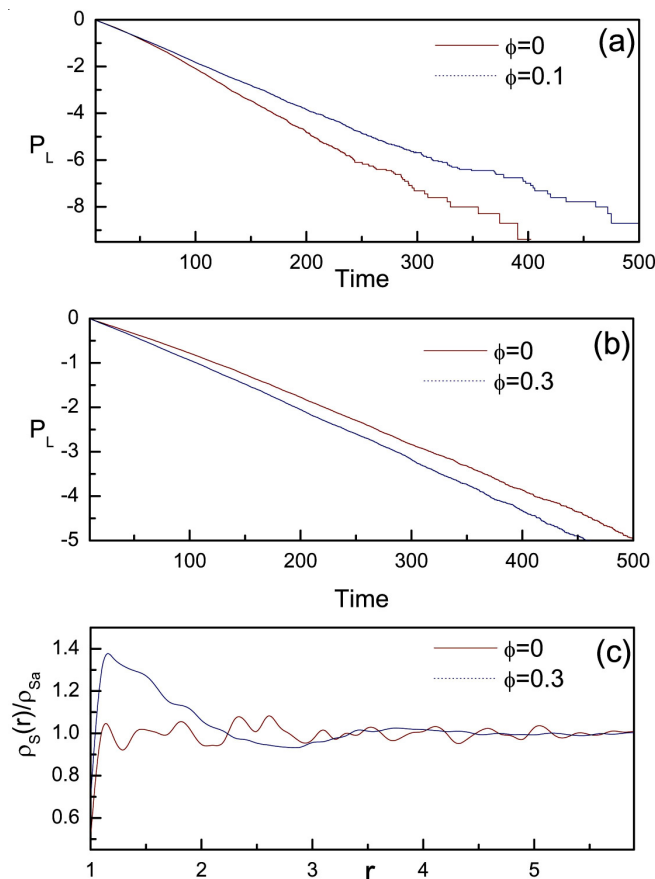


Fig. 4. Survival probability of substrate as a function of time for (a) $r_s = 0$ (b) $r_s = 1.0$ with different volume fraction of obstacle. (c) Relative density of substrate molecules as a function of radial distance from enzyme. $\rho_{s,a}$ is the averaged density of substrate in the bulk of the system. The reaction rate is $k_2 = 0.8$ and $k_1 = 0.01$

Due to the influence of diffusion effect of reactants, the reaction rate coefficient $k_1(t)$ shows time dependent instead of constant value. $k_1(t)$ can be defined by the rate law:

$$\frac{d\rho_C}{dt} = k_1(t)\rho_E\rho_S - (k_{-1} + k_2)\rho_C \quad (11)$$

Then, the value of $k_1(t)$ can be obtained through calculating:

$$k_1(t) = \frac{d\gamma(t)/dt}{\rho_E\rho_S} \quad (12)$$

where $\gamma(t)$ related to k_1 by:

$$\gamma(t) = \int_0^t k_1(t')\rho_E(t')\rho_S(t')dt' \quad (13)$$

is the total number of enzyme-substrate collisions that have effectively given rise to complex formation⁶ after time t . In

Fig. 5, we plot the $k_1(t)$ with different volume fraction of obstacle and size of substrate.

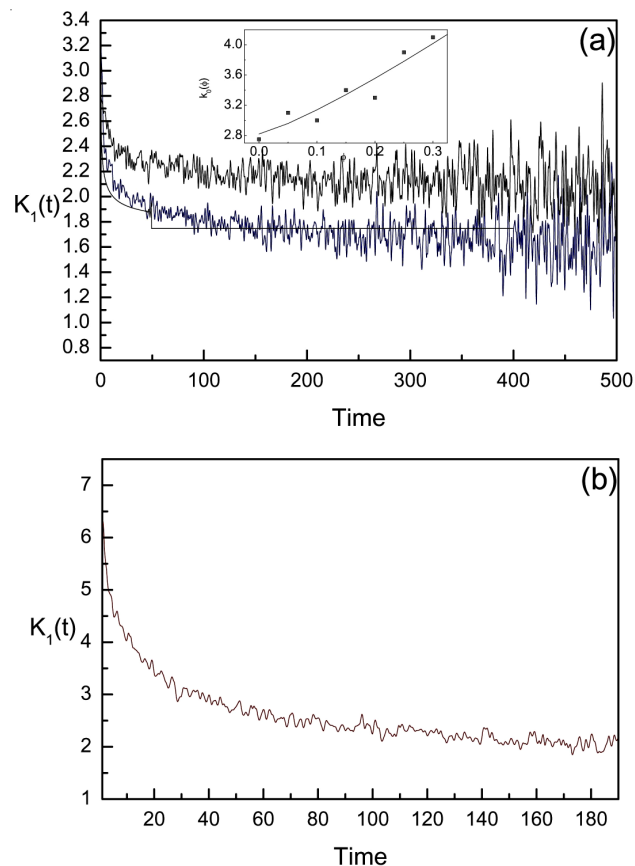


Fig. 5. Evolution of $k_1(t)$ with varying ϕ and r_s . (a) $r_s = 0$. The dotted line and dashed line indicates $\phi = 0$ and $\phi = 0.2$, respectively. The solid line shows theoretical result from eqn. 16. (b) $r_s = 0.5$, $\phi = 0.2$

Firstly, we discuss the value of $k_1(0)$. We get $k_1(0) = 2.78$ from simulation in Fig. 5 as $r_s = 0$ and $\phi = 0$. This value is consistent with theoretical estimation $k_1(0) = 2.82$ from the function²⁵.

$$k_1(0) = p_R \left(\frac{8\pi k_B T}{\mu_{ES}} \right)^{\frac{1}{2}} r_c^2 \quad (14)$$

For the increase of obstacles leads to the density of the substrate near the enzyme higher than that in the bulk of the system, the $k_1(0)$ also shows ϕ dependence. In the calculation from function (14), the value of ρ_s is the averaged density that is smaller than the actual value near the enzymes, which make $k_1(0)$ increased with ϕ . An example of $k_1(t)$ with $\phi = 0.2$ is shown in Fig. 5(a). We change the value of ϕ and plot the corresponding value of $k_1(0)$ in the inset of Fig. 5(a). The fit solid line indicates a relation.

$$k_1(0, \phi) = k_1(0)(1 + a\phi^b) \quad (15)$$

with $a = 1.8$ and $b = 1.2$. This relation is also confirmed by the case with $r_s = 0.5$ and $\phi = 0.2$ in Fig. 5(b), where, $k_1(0)$ is about 7.6 while its value is 8.0 from function (14) by replacing $r_c = 2^{1/6}r_E$ with $r_c = 2^{1/6}(r_E + r_s)$.

The evolution of $k_1(t)$ in Michaelis-Menten reaction is difficult to get from theoretical analysis. In order to show qualitative information, we compare our simulation result with theoretical result plotted from the reaction $E + S \rightarrow E + P$ ²⁶.

$$k_1(t) = \frac{k_1^0 k_D}{k_1^0 + k_D} + \frac{(k_1^0)^2}{k_1^0 + k_D} \exp\left[\left(1 + \frac{k_1^0}{k_D}\right)^2 \frac{Dt}{r_{EE}^2}\right] \times \operatorname{erfc}\left[\left(1 + \frac{k_1^0}{k_D}\right) \left(\frac{Dt}{r_{EE}^2}\right)^{1/2}\right] \quad (16)$$

This expression for $k_1(t)$ is obtained when the diffusion equation is solved subject to the radiation boundary condition, $k_1(0)\rho_s(r_{EE}, t) = 4\pi r_{EE}^2 D \hat{r} \cdot \nabla \rho_s(\bar{\sigma}_E, t)$, where $\rho_s(r, t)$ is the local substrate density at a distance r from the enzyme and \hat{r} is unit radial vector. In fig. 5(a), one obvious result is that the fall of $k_1(t)$ is slower in Michaelis-Menten reaction. It can be rationalized by the different reaction kinetic. In reaction $E + S \rightarrow E + P$, the S substrates continually becomes P product as they encounter E with fast decrease of substrate density near E. Consequently, gradient of substrate density near enzyme is formed. However, substrates in Michaelis-Menten should compete with each other to get the chance forming complex. At one time, only one substrate can succeed in associating with one enzyme and others are pushed back from the occupied enzymes. It needs time to wait for the disassociation of the complex again so that $E + S \rightarrow C$ can occur again, which moderates the gradient near enzyme by diffusing of substrate. Thus, the $k_1(t)$ in reaction $E + S \rightarrow E + P$ falls faster and its value at the same time is smaller than that in Michaelis-Menten. In terms of this discussion, it is clear that the decrease of diffusion coefficient of substrate in Michaelis-Menten may induces higher gradient and leads to faster decrease of $k_1(t)$. One can find this point by comparing the curves with $\phi = 0$ and $\phi = 0.2$ in Fig. 5(a). Certainly, the increase of substrate size greatly decreases the diffusion coefficient and results in fast decreasing of $k_1(t)$, which can be seen in Fig. 5(b). The $k_1(t)$ approaches²⁴.

$$k_1(\infty) = \frac{k_1(0)k_D}{k_1(0) + k_D} \quad (17)$$

In the long time. We get $k_1(\infty) = 1.86$ ($\phi = 0$) and $k_1(\infty) = 1.61$ ($\phi = 0.2$), which is slight bigger than that from theoretical function (17) where $k_1(\infty)$ is 1.75 ($\phi = 0$) and $k_1(\infty)$ 1.59 ($\phi = 0.2$) respectively. We attribute the slight increase to the cooperative reaction from the reaction network formed by many enzymes possessing other rebind P_O . To the case with $r_s = 0.5$, It is found that the simulated $k_1(1)$ is about 1.8 which is bigger than the value 0.98 from the calculation (17). We attribute the result to the obvious increase of probability of self rebind P_S . The first collision and other rebind P_O are predominated by diffusion which is characterized by D. These influences have been taken into account in D, k_D and then $k_1(\infty)$. However, the contribution of self rebind P_S has not been consider in $k_1(\infty)$ (17). Thus, the calculated $k_1(\infty)$ is smaller than the simulation result.

Conclusion

In conclusion, we have studied the Michaelis-Menten scheme of enzyme-network kinetics in crowded environment

through a particle-based stochastic model based on a mesoscopic hybrid molecular dynamics-multiparticle collision (MD-MPC) dynamics method. Nontrivial effects are observed due to the compartmentalization of big substrate induced by crowded obstacles and cooperative reaction from enzyme-network. The simulated diffusion coefficient of point-like substrate molecule is in accord with theoretical calculation when volume fraction of obstacle is increased, while D of big substrate shows strong nonlinearity. When the volume fraction of obstacles increases, the self rebind and other rebind probability of big substrate increases and decreases fast, respectively. The survival probability of big substrate increases as volume fraction of obstacles while small substrate shows opposite tendencies. We studied the time dependent reaction rate $k_1(t)$ in three regimes, that is $k_1(0)$, evolution of $k_1(t)$ and $k_1(\infty)$. The results are compared with theoretical results and discussed. We hope our results can shed light on enzyme kinetics in complex environment.

ACKNOWLEDGEMENTS

The authors are grateful to J.X. Chen for useful discussions. This work was supported by the National Nature Science Foundation of China (Nos. 10747120).

REFERENCES

1. A. Fulton, *Cell*, **30**, 345 (1982); D.S. Goodsell, *Trends Biochem. Sci.*, **16**, 203 (1991).
2. G. Guigas, C. Kalla and M. Weiss, *Biophys. J.*, **93**, 316 (2007).
3. G. Rivas, J.A. Fernandez and A.P. Minton, *Biochemistry*, **38**, 9379 (1999).
4. G. Rivas, J.A. Fernandez and A.P. Minton, *Proc. Natl. Acad. Sci., USA* **98**, 3150 (2001).
5. B. van den Berg, R. Wain, C.M. Dobson and R.J. Ellis, *EMBO J.*, **19**, 3870 (2000).
6. H. Berry, *Biophys. J.*, **83**, 1891 (2002).
7. D. Banks and C. Fradin, *Biophys. J.*, **89**, 2960 (2005).
8. I. Golding and E. Cox, *Phys. Rev. Lett.*, **96**, 098102 (2006).
9. M. Agrawal, S.B. Santra, R. Anand and R. Swaminathan, *Pramana J. Phys.*, **71**, 359 (2008).
10. U. Kettling, A. Koltermann, P. Schuille and M. Eigen, *Proc. Natl. Acad. Sci. USA*, **95**, 1416 (1998).
11. S. Park and N. Agmon, *J. Phys. Chem. B*, **112**, 5977 (2008).
12. H.X. Zhou, *J. Phys. Chem. B*, **101**, 6642 (1997).
13. A.V. Popov and N. Agmon, *Chem. Phys. Lett.*, **340**, 151 (2001).
14. N. Malchus and M. Weiss, *J. Fluoresc.*, **20**, 19 (2010).
15. R. Grima, *J. Chem. Phys.*, **132**, 185102 (2010); R. Grima, *BMC Systems Biol.*, **3**, 101 (2009).
16. S. Schnell and T.E. Turner, *Prog. Biophys. Mol. Biol.*, **85**, 235 (2004).
17. J.S. Kim and A. Yethiraj, *Biophys. J.*, **96**, 1333 (2009).
18. B.J. Sung and A. Yethiraj, *J. Chem. Phys.*, **123**, 114503 (2005).
19. M. Litniewski, *J. Chem. Phys.*, **123**, 124506 (2005).
20. C. Echeverria and R. Kapral, *J. Chem. Phys.*, **132**, 104902 (2010).
21. G. Gompfer, T. Ihle, D.M. Kroll and R.G. Winkler, *Adv. Polym. Sci.*, **221**, 1 (2009).
22. S. Thakur, J.X. Chen and R. Kapral, *Angew. Chem. Int. Ed.*, **50**, 10165 (2011).
23. D. Gillespie, *J. Phys. Chem.*, **81**, 2340 (1977).
24. J.X. Chen and R. Kapral, *J. Chem. Phys.*, **134**, 044503 (2011).
25. R. Kapral, *Adv. Chem. Phys.*, **140**, 89 (2008).
26. J. Lebenhaft and R. Kapral, *J. Stat. Phys.*, **20**, 25 (1979).